Bulletin of Mathematical Biology (2009) 71: 863–887
DOI 10.1007/s11538-008-9385-3

ORIGINAL ARTICLE

Excitable Population Dynamics, Biological Control Failure, and Spatiotemporal Pattern Formation in a Model Ecosystem

Andrew Morozov, Sergei Petrovskii*

Department of Mathematics, University of Leicester, Leicester LE1 7RH, UK

Received: 11 June 2008 / Accepted: 2 December 2008 / Published online: 24 December 2008

Abstract Biological control has been attracting an increasing attention over the last two decades as an environmentally friendly alternative to the more traditional chemical-based control. In this paper, we address robustness of the biological control strategy with respect to fluctuations in the controlling species density. Specifically, we consider a pest being kept under control by its predator. The predator response is assumed to be of Holling type III, which makes the system's kinetics "excitable." The system is studied by means of mathematical modeling and extensive numerical simulations. We show that the system response to perturbations in the predator density can be completely different in spatial and non-spatial systems. In the nonspatial system, an overcritical perturbation of the population density results in a pest outbreak that will eventually decay with time, which can be regarded as a success of the biological control strategy. However, in the spatial system, a similar perturbation can drive the system into a self-sustained regime of spatiotemporal pattern formation with a high pest density, which is clearly a biological control failure. We then identify the parameter range where the biological control can still be successful and describe the corresponding regime of the system dynamics. Finally, we identify the main scenarios of the system response to the population density perturbations and reveal the corresponding structure of the parameter space of the system.

Keywords Biological control · Predator-prey system · Holling type III · Excitable system · Excitability · Pattern formation

1. Introduction

Mathematical models of population dynamics are of considerable interest because of their proven power to make important insights into the dynamics of real populations and communities (May, 1974; Nisbet and Gurney, 1982; Murray, 1989; Shigesada and Kawasaki,

*Corresponding author.
E-mail address: sp237@le.ac.uk (Sergei Petrovskii).
A. Morozov is on leave from Shirshov Institute of Oceanology, Russian Academy of Science, Nakhimovsky Prosp. 36, Moscow 117218, Russia.

1997). Much has been learned through the application of mathematical modeling. In particular, the idea of intrinsic population cycles, which is one of the basic concepts of contemporary theoretical ecology, would hardly have ever appeared without the mathematical work by Lotka (1925) and Volterra (1926).

While the original idea of population cycles was obtained in terms of a simple bilinear model, later studies showed that the details of the system "kinetics" are important. Introduction of saturation into species growth leads to the limit-cycle oscillations which are biologically more relevant than neutral stability of the Volterra model. Later, there came the recognition that even smaller details can have a crucial effect. In a predator-prey system where predation is described by a concave function, cf. Holling type II trophic response, population cycles appear when the equilibrium state looses its stability through the Hopf bifurcation. Stationary species coexistence is then not possible any more and the large-time system dynamics is given by periodic population oscillations that can be of various amplitude for different parameter values, ranging from very small to very large.

On the contrary, a predator-prey system with a sigmoid-shaped predator response, cf. Holling type III, exhibits properties similar to what is known as an "excitable system": a sufficiently large perturbation of the locally-stable coexistence state results in a single population cycle of large amplitude. When the system returns, in the large-time limit, into its steady state it stays there until another supercritical perturbation will drive it away. This model is therefore more appropriate to describe population outbreaks rather than periodical self-sustained cycles. Indeed, it was originally used to describe spruce budworm outbreaks in forest ecosystems (Ludwig et al., 1978), and later to study the "red tides" in marine plankton communities (Truscott and Brindley, 1994a, 1994b).

An issue that has been a challenging problem for ecology over several decades is harmful species management. Application of chemical pesticides which used to be the main tool of control is currently regarded as ineffective because its nonselective impact on harmful and nonharmful species as well as on humans. Alternatively, an increasing attention has been recently paid to a possibility of biological control (Fagan et al., 2002; Sapoukhina et al., 2003; Briggs and Hoopes, 2004; Hajek, 2004) which is based on the assumption that the abundance of given species is likely to become lower in the presence of its competitors and/or predators or parasites. Indeed, there are many examples when this strategy has been successfully implemented in practice, e.g., see Room et al. (1981), McEvoy et al. (1991) and Mendel et al. (1998).

A broader practical application of biological control requires better understanding of the limits of its robustness with respect to fluctuations in the species densities. It is intuitively clear that to keep given harmful species under control, the density of the controlling agent, e.g., its predator, should be sufficiently high. However, what actually can happen if the predator density falls to a low value, e.g., as a result of a fluctuation in the weather conditions or unintentional anthropogenic impact? Apparently, the answer depends on the type of the species interaction. While for a nonspatial system with Holling type II predator response to a perturbation in population density will promptly decay with time, for a population system with excitable kinetics a perturbation of the same magnitude may result in a population outbreak. In the latter case, the system then eventually returns into its equilibrium state, but not until after its trajectory in the corresponding phase space makes a long "excursion" through the domains where the population density can be very high.

The above problem is much less understood if considered in space. Several papers have been published to address the issue of population outbreaks, cf. Ludwig et al. (1978), Harrison (1997), and Hunter and Dwyer (1998); however, they were mostly concerned with

the temporal dynamics leaving the spatial aspect of the phenomenon aside (but see Petrovskii and Li, 2001). Meanwhile, the spatial aspect makes the systems dynamics notably richer and often qualitatively different, bringing phenomena that are not possible in the corresponding homogeneous system, i.e., spatial/spatiotemporal pattern formation (Pascual, 1993; Pascual and Caswell, 1997; Sherratt et al., 1995; Petrovskii and Malchow, 1999, 2001; Malchow et al., 2008). Therefore, an immediate question is how a local population outbreak in an excitable predator-prey system, which can be triggered by an accidental change in the population density, will evolve in space and time. In particular, an issue that is important for credibility of the biological control strategy as a whole is whether the original equilibrium state of the system is going to be restored or the perturbation may drive the system into a self-sustained dynamical regime.

In this paper, we address this issue by means of mathematical modeling and extensive computer simulations. We show that compared to the corresponding nonspatial system, a spatially extended predator-prey system with excitable kinetics can have an essentially different type of response to a perturbation of species density. While in a homogeneous system a population outbreak eventually decays with time, so that the system gradually returns to its locally stable steady state, in the corresponding spatial system a localized perturbation may result in a self-sustained spatially heterogeneous structure. We also show that the conditions of successful biological control appear to be restricted to the case when diffusivity of the harmful species (i.e., prey) is on the same order as the diffusivity of its predator, while both very fast and very slow species are able to escape. Finally, we identify the main regimes of the system dynamics and reveal the structure of the parameter space of the system.

2. Main equations

The spatiotemporal dynamics of a harmful species U, being controlled by its predator V, is described by the following model:

$$\frac{\partial U(X,Y,T)}{\partial T} - D_1\nabla^2 U = F(U) - G(U)V, \tag{1}$$

$$\frac{\partial V(X,Y,T)}{\partial T} - D_2\nabla^2 V = \kappa G(U)V - MV, \tag{2}$$

where U and V are the densities of prey and predator, respectively, at moment T and position (X, Y), D_1 and D_2 are species diffusivities due to the motion of individuals and κ is the prey consumption efficiency. Function $F(U)$ describes prey reproduction, the term $G(U)V$ describes predation, and the term MV stands for predator mortality.

It should be mentioned that Eqs. (1–2) can be regarded as a simple ecosystem model where prey is a producer and predator is a consumer. The impact of other trophic levels and environmental factors is taken into account through the corresponding coefficient values; for instance, the per capita mortality rate M may describe a combined effect of the natural mortality and the predation by a top predator (cf. Scheffer, 1991, 1998).

We consider Holling type III predator trophic response and use the following parametrization:

$$G(U) = A\frac{U^2}{B^2 + U^2}, \tag{3}$$

where A describes predation intensity and B is the half-saturation prey density.

For the prey reproduction, we assume that it can be described by the logistic growth function:

$$F(U) = rU\left(1 - \frac{U}{K}\right), \tag{4}$$

where K is the prey carrying capacity and r is the maximum *per capita* growth rate.

Introducing dimensionless variables, $u = U/K$, $v = V/(\kappa K)$, $x = X(a/D_2)^{1/2}$, $y = Y(a/D_2)^{1/2}$ and $t = aT$ where $a = A\kappa K^2 B^{-2}$, from Eqs. (1–4), we obtain:

$$\frac{\partial u(x,y,t)}{\partial t} - \epsilon\nabla^2 u = \gamma u(1-u) - \frac{u^2 v}{1+\alpha^2 u^2}, \tag{5}$$

$$\frac{\partial v(x,y,t)}{\partial t} - \nabla^2 v = \frac{u^2 v}{1+\alpha^2 u^2} - \mu v, \tag{6}$$

where $\alpha = K/B$, $\gamma = r/a$, $\mu = M/a$ and $\epsilon = D_1/D_2$.

Along with system (5–6), we consider its 1-D analogue, i.e.,

$$\frac{\partial u(x,t)}{\partial t} - \epsilon\frac{\partial^2 u}{\partial x^2} = \gamma u(1-u) - \frac{u^2 v}{1+\alpha^2 u^2}, \tag{7}$$

$$\frac{\partial v(x,t)}{\partial t} - \frac{\partial^2 v}{\partial x^2} = \frac{u^2 v}{1+\alpha^2 u^2} - \mu v. \tag{8}$$

Most of the results below will be obtained by means of numerical simulations. For that purpose, we need specific choice of the prey growth function and the predator trophic response, cf. Eqs. (3–4). However, we will also make use of some results that can be proved rigorously and for a rather general case, when parametrization is not specified. Thus, along with (5–6), we will also retain a more general form for the predator-prey system:

$$\frac{\partial u}{\partial t} - \epsilon\nabla^2 u = f(u) - g(u)v \equiv P(u,v), \tag{9}$$

$$\frac{\partial v}{\partial t} - \nabla^2 v = g(u)v - \mu v \equiv Q(u,v), \tag{10}$$

where, for biological reasons, $g(u)$ is a monotonously increasing function, $g(0) = 0$, $g(u) > 0$ for $u > 0$. Apparently, the system (9–10) has the same structure as the original system (1–2) but all the values are now dimensionless.

Before proceeding to the spatially explicit case, it is useful to have a look at the properties of the local dynamics, i.e., at the properties of the following system:

$$\frac{du}{dt} = f(u) - g(u)v, \qquad \frac{dv}{dt} = g(u)v - \mu v. \tag{11}$$

The (null-)isoclines of the system (11) are given by the following equations:

$$\text{(a)} \quad v_1(u) = \frac{f(u)}{g(u)} \quad (u > 0) \quad \text{and} \quad \text{(b)} \quad g(\bar{u}) = \mu. \tag{12}$$

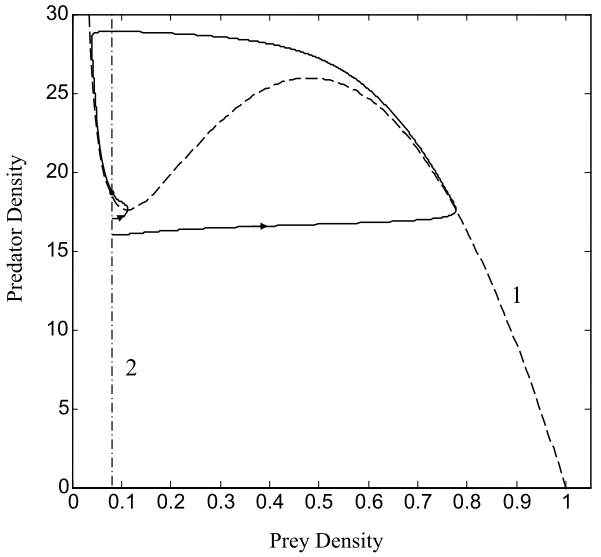

Fig. 1 Phase plane of the system (11) shown for $\alpha = 10$, $\gamma = 1$ and $\mu = 0.004$. Curves 1 and 2 show the isoclines; solid curves show different system's trajectories for the initial perturbation of different magnitude, smaller loop for a subcritical initial perturbation, larger loop for an overcritical initial perturbation.

Since function $g(u)$ is monotonously increasing, the last equation in (12) provides a unique value $\bar{u}$.

In the case of the specific parameterizations considered above, it turns into

$$v_1(u) = \frac{\gamma}{u}(1-u)\big(1+\alpha^2 u^2\big), \tag{13}$$

and

$$u = \bar{u} = \left(\frac{\mu}{1-\mu\alpha^2}\right)^{1/2}, \tag{14}$$

respectively.

The shape of the isocline $v_1(u)$ appears to essentially depend on parameter α. While for small values of α, it is a monotonously decreasing function, for $\alpha^2 > \alpha_c^2 = 27$, it acquires two local extremuma, so that the corresponding curve becomes S-shaped. The corresponding phase plane of the system is shown in Fig. 1. Note that parameter μ affects only the position of the isocline $u = \bar{u}$ but not the shape or position of $v_1(u)$.

It is readily seen that apart from the extinction state $(0, 0)$ and the prey-only state $(1, 0)$, system (11) can have only one coexistence steady state which is feasible for

$$\mu < \frac{1}{1+\alpha^2}. \tag{15}$$

Note that the prey density $\bar{u}$ in the coexistence state can be significantly lower than it would be without predator. This simple observation makes a theoretical beachhead for bi-

ological control strategy: an introduction of a relevant predator can make the pest density much smaller.

The next issue is the steady state stability. It is straightforward to check that the extinction state $(0, 0)$ is always unstable. The prey-only state $(1, 0)$ is unstable when the isocline for predator, cf. (14), crosses the u-axis on the left of $u = 1$, i.e., under condition (15); otherwise, the state $(1, 0)$ is stable. Correspondingly, it means that the prey-only state becomes stable only when the coexistence state(s) goes below the horizontal axis and, therefore, disappears from the upper semiplane.

As for the stability of the coexistence state $(\bar{u}, \bar{v})$, it depends on the position of the state with respect to the local extremuma of the null-isocline $v_1(u)$. The coexistence steady state is stable if and only if the vertical line (12b) crosses a descending part of the prey isocline $v_1(u)$. In particular, it means that it is always stable for $\alpha^2 < \alpha_c^2$.

The standard linear stability analysis gives conditions of steady state stability with respect to small perturbations. An important question is what can be the system's response if a perturbation is not small. A generic property of excitable systems (e.g., see Murray, 1989) is that there exists a threshold value of the density perturbations, so that a perturbation of an overcritical amplitude will not decay straightforwardly. Instead, at the first stage, the prey density may exhibit an exponentially fast growth up to very large values. At the second stage, the prey density starts decreasing at a slow rate, which is then followed by a fasts decay, and finally by a slow relaxation to its original steady state value. The corresponding system's trajectory is shown in Fig. 1 by the long solid curve; for comparison, the short solid curve corresponds to the fast decay of small (subcritical) perturbations.

3. Regimes of spatiotemporal dynamics

Excitable systems have been under intensive study for about 3 decades in relation to various physical, chemical, and biological phenomena (Fife, 1976; Murray, 1989; Pearson, 1993; Krischer and Mikhailov, 1994; Muratov and Osipov, 1996a, 1996b; Ermentrout et al., 1997; Gurney et al., 1998). Yet the principal issue of identification of the main spatiotemporal self-organization scenarios in such systems is still very far from being addressed exhaustively. One apparent reason for that is that a regular analytical study of a system of diffusion-reaction equations is virtually impossible, subject to only a few exceptions (cf. Mimura et al., 1980; Muratov and Osipov, 1996a). Analytical approaches are usually limited to the case when the ratio of the diffusion coefficients is either very small, $\epsilon \ll 1$, or very large, $\epsilon \gg 1$. Even in these cases, however, existing analytical approaches typically result not in a problem solution or a bifurcation diagram or a dispersion relation, but just in a somewhat simpler system of differential equations, which still needs to be solved numerically (Muratov, 1996).

Surprisingly enough, also direct numerical simulations of the original system have usually been restricted to the case $\epsilon \ll 1$ (cf. Muratov and Osipov, 1996b) while system's properties for $\epsilon \sim 1$ remain largely nonaddressed. That leaves a wide gap in our knowledge. In order to bridge this gap (at least, partially) and to reveal the corresponding succession of dynamical regimes, in this study, we fulfilled extensive numerical simulations varying ϵ from 0 to the values on the order of 1.

Let us note that the system under study depends on four parameters. Therefore, its exhaustive numerical investigation, i.e., by varying each of the parameter in a sufficiently

wide range, is hardly possible. Instead, we applied another strategy. Namely, we fulfilled a detailed study varying only two of the parameters and keeping the other two fixed at a certain hypothetical value.

In order to appropriately choose the parameters to be varied, we have to take into account some biological arguments along with a priori information about the system properties. A motivation of this study has been found in the problem of biological control, the controlling factor being assumed to be predation. Intensity of predation can be regulated by means of varying predator mortality; thus, a relevant controlling parameter is μ. On the other hand, the properties of a diffusion-reaction system are known to depend significantly on the diffusivity ratio; correspondingly, the second parameter to be varied is ϵ.

Equations (5–6) and (7–8) were solved by the finite difference method using an implicit numerical scheme for the 1-D system and a simple explicit scheme for the 2-D system (Thomas, 1995). Sensitivity of the results to the value of the grid steps in space and time was checked and their values were chosen sufficiently small in order to avoid any significant numerical artifact. At the boundaries of the numerical domain, the no-flux conditions were applied.

For the initial conditions, we assume that perturbation of the equilibrium state originally takes place in a certain finite domain. Moreover, here we are mostly interested in the situation when only the predator density is perturbed (decreased). Specifically, we consider the initial conditions in the following form:

$$u(x,0) = \bar{u} \quad \text{for any } x, \tag{16}$$

$$v(x,0) = V_0 < \bar{v} \quad \text{for } -\Delta_v < x < \Delta_v, \quad \text{otherwise} \quad v(x,0) = \bar{v} \tag{17}$$

in the 1-D case, and

$$u(x,y,0) = \bar{u} \quad \text{for any } (x,y), \tag{18}$$

$$\begin{aligned} &v(x,y,0) = V_0 + a(x-x_0) + b(y-y_0) \\ &\quad \text{for } |x-x_0| < \Delta_x \quad \text{and} \quad |y-y_0| < \Delta_y, \quad \text{and} \\ &v(x,y,0) = \bar{v} \quad \text{otherwise}, \end{aligned} \tag{19}$$

in the 2-D case. Here, V_0 is the initial value of the (perturbed) predator density, Δ_v or Δ_x and Δ_y give the size of the affected domain, and a and b are auxiliary parameters with an obvious meaning.

It should be mentioned that the type of system's dynamics crucially depends on the "magnitude" of the initial outbreak, i.e., on the initial density perturbation $|V_0 - \bar{v}|$ and the size of the domain (i.e., Δ_v or Δ_x and Δ_y). In a spatially extended excitable system, in case the size is not large enough, an initial perturbation will decay promptly and the spatially homogeneous steady state is retained, even if the value of $|V_0 - \bar{v}|$ would be sufficient to trigger a population outbreak in the nonspatial case. An interesting problem here would be to estimate the critical parameter values separating different regimes (cf. "the problem of critical aggregation," Petrovskii and Li, 2006); however, it lies beyond the scope of this paper. Since here we are more interested in a nontrivial spatiotemporal evolution of the initial outbreak, in our simulations, the initial density perturbation and the size of the perturbed domain are always chosen to be sufficiently large.

3.1. Pattern formation in 1-D case

One issue to be addressed before proceeding to simulations is how to choose the parameter values compatible with those of real populations. It should be mentioned here that depending on particular system, the range of possible values span over almost two orders of magnitude. For instance, while for the rodents-weasels system the value of $\alpha = K/B$ is roughly estimated to be between 5–6 (cf. Sherratt and Smith, 2008), for a phyto-zooplankton system it is between 10–20 (Truscott and Brindley, 1994a; Franks, 2001), and for the budworm-birds system it is on the order of 100 (Ludwig et al., 1978). A related question is then whether thew system's kinetics is actually excitable. Since the plankton system has long been one of the paradigms of the excitable population dynamics (Truscott and Brindley, 1994a,1994b), we chose it as a prototype and look for the other parameter values accordingly, which are estimated as $r = 1$–2 day^{-1} (Edwards and Brindley, 1999), $A\kappa = 0.03$–0.06 day^{-1} (Truscott and Brindley, 1994a; Edwards and Brindley, 1999) and $M = 0.01$–0.02 day^{-1} (Truscott and Brindley, 1994a), so that $\gamma = 0.04$–0.7 and $\mu = 0.0004$–0.007.

Correspondingly, in order to investigate possible dynamical regimes of the system (7–8) in computer simulations, we fix $\alpha = 10$ and $\gamma = 1$. With these values, the system's kinetics is excitable; see Fig. 1. We then run our code for different combinations of μ and ϵ, each of them being consequently varied in a wide range. For all parameter values, we have used the initial conditions (16–17) with $V_0 = 16$ and $\Delta_v = 2.5$. Basing on the results obtained in this way, we then construct a parametric portrait in the (μ, ϵ) plane, see Fig. 2, with the examples of different regimes shown in Figs. 3, 4, 5.

For large values of ϵ (domain 1 in Fig. 2), a local disturbance of the homogeneous equilibrium results in the formation of a solitary traveling patch or "pulse." Figure 3a

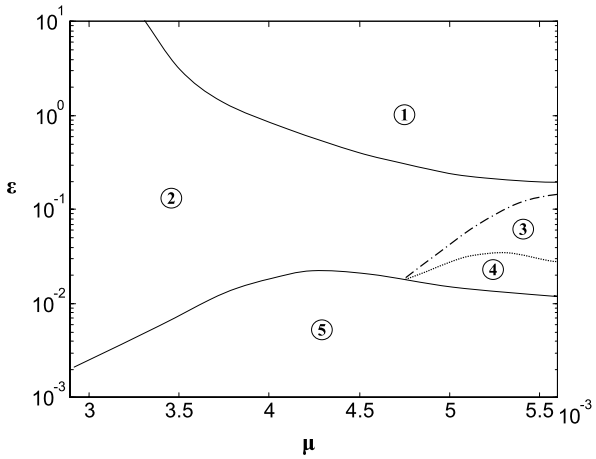

Fig. 2 A map in the $\mu - \epsilon$ parameter plane obtained for $\gamma = 1$ and $\alpha = 10$ and the initial conditions $V_0 = 16$ and $\Delta_v = 2.5$. Different domains correspond to different dynamical regimes of the system: domain 1 for the traveling patches or "pulses" (Fig. 3a), domain 2 for the pulses localization (Fig. 3b), domain 3 for the formation of irregular patchy pattern (Fig. 4), domain 4 for the formation of periodic spatial pattern and domain 5 for the formation of a solitary standing patch (Fig. 5a).

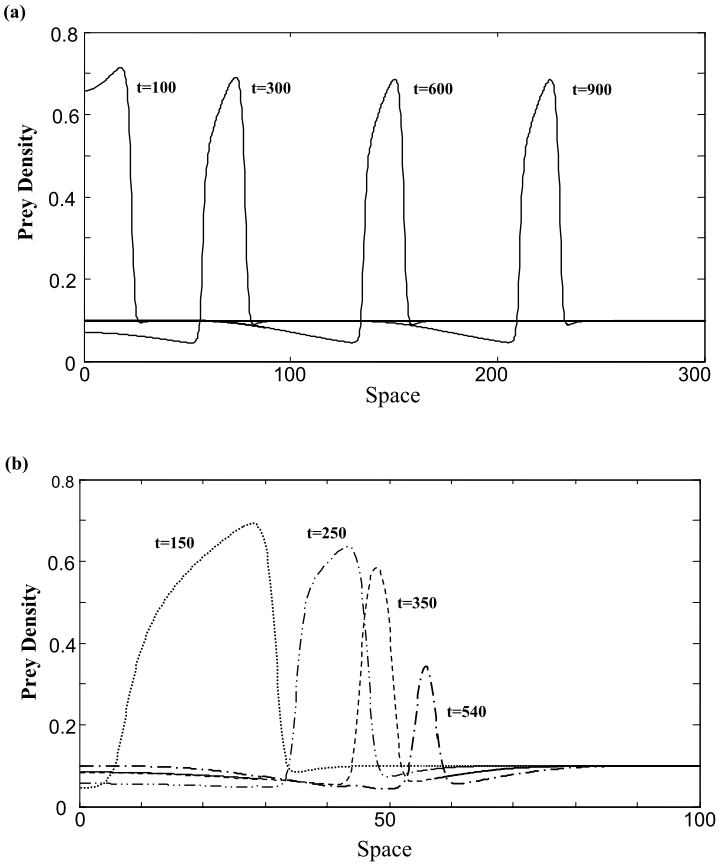

Fig. 3 Snapshots of the prey population density. (a) Traveling patches/pulses propagation shown for $\mu = 0.005$ and $\epsilon = 0.3$. (b) The dynamical localization of the pulses due to the catch-up of the predator; parameters are $\mu = 0.005$ and $\epsilon = 0.2$.

shows snapshots of the prey population density (the predator density forms a qualitatively similar pattern) calculated at different moments of time for $\mu = 0.005$ and $\epsilon = 0.3$. Correspondingly, $\bar{u} = 0.1$ and $\bar{v} = 18$. Since the problem is symmetrical with respect to the origin, in Figs. 3–5 only half of the whole numerical domain is shown. The pulse propagates with a constant speed and its shape remains unchanged. In the wake of the pulse, the homogeneous species distribution is eventually restored. The underlying mechanism of the pulse propagation is qualitatively similar to a prey-predator pursuit mechanism (cf. Murray, 1989). We want to mention that this type of spatiotemporal dynamics is very common for the systems with excitable kinetics, e.g., see Muratov and Osipov (1996b); also Lindner et al. (2004) and references therein.

However, for somewhat smaller values of prey dispersal rate (domain 2 in Fig. 2), the predator becomes capable to catch up with the prey and to bring it down. Figure 3b shows snapshots of the prey density at different moments of time for the parameters $\mu = 0.005$ and $\epsilon = 0.2$. At the early stage, a traveling population pulse is formed. The pulse prop-

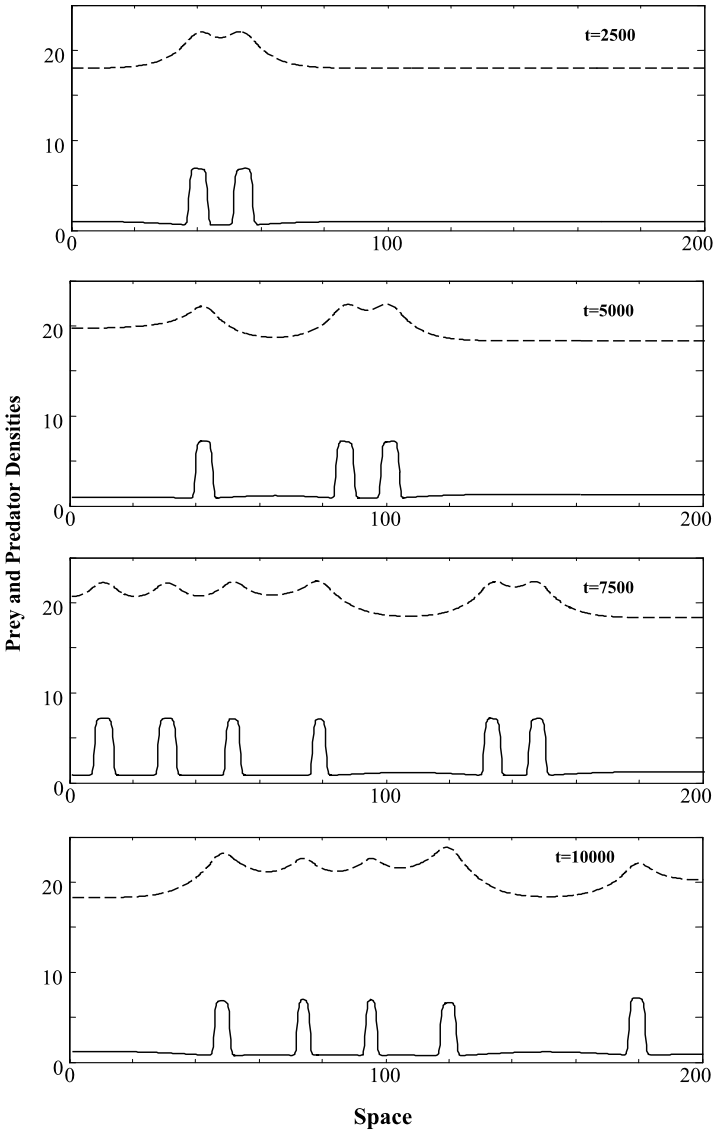

Fig. 4 Snapshots of the population density (solid curve for prey, dashed for predator): Formation of an irregular spatial pattern for parameters $\mu = 0.005$ and $\epsilon = 0.03$.

agates over a certain distance with almost constant speed. However, these dynamics are now not self-sustained. The predator finally catches up with the prey; the pulse is blocked and the outbreak disappears promptly. This change in the pattern of dynamics coincides very well with what is intuitively expected basing on ecological argument. A decrease in ϵ means that prey is a slower moving species compared to predator, and thus it becomes more vulnerable, cf. Fagan et al. (2002) and the references therein.

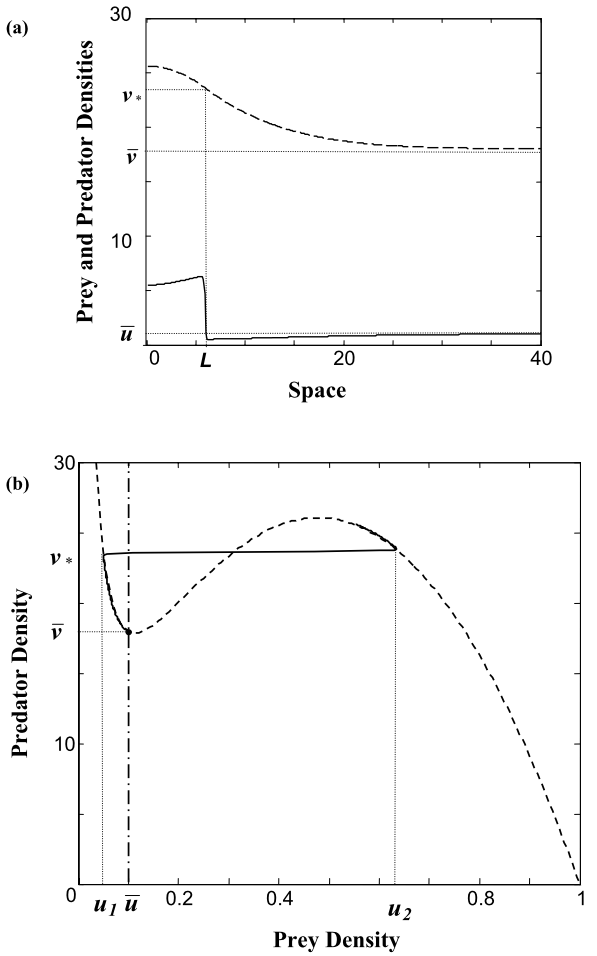

Fig. 5 (a) A snapshot of the population density (solid curve for prey, dashed for predator) in the case of a solitary stationary patch, parameters are $\mu = 0.005$ and $\epsilon = 0.001$. The vertical dashed-and-dotted line shows the position of the patch boundary. (b) The phase plane of the system, the thick curve (partially coinciding with the isocline) corresponds to a discontinuous population density profile obtained in the limiting case $\epsilon = 0$.

Surprisingly, a further decrease in the diffusivity ratio ϵ results in regimes where the prey is able to escape again. In particular, Fig. 4 shows the snapshots of the population densities obtained for $\mu = 0.005$ and $\epsilon = 0.03$ (domain 3). Population patches now spread over whole domain forming an irregular spatial pattern. The motion of patches is more complicated than the simple propagation in the case of a traveling pulse. The patches interact with each other, merge and split; some of them may disappear but new patches are formed instead, etc. The area occupied by patches grows in size steadily so that finally, the irregularly moving interacting patches occupy the whole domain. Long-term simulations

prove that this regime of the system dynamics is self-sustained, and the system never returns to its spatially homogeneous state.

For lower values of ϵ (see domain 4), the localized initial perturbation also spreads over the whole domain through the dynamics of separate patches but leading to a somewhat different result. (For the sake of brevity, we do not show the corresponding snapshots here.) In this case, the final spatial population distribution forms a structure that is stationary and periodical in space. The total number of the patches is determined by the length L of the area. Formation of this type of pattern is usually attributed to Turing's instability. In our case, however, the mechanism is different. Indeed, it is readily seen that in a predator-prey system with a prey-dependent predator trophic response[1] and a linear predator mortality, the conditions for Turing's instability cannot be fulfilled; see Segel and Jackson (1972), also Malchow et al. (2008) for more details.

For very small values of ϵ (domain 5), the predator becomes able to catch up with the prey again. However, the predator can now only block the propagation of the outbreak but cannot bring it down, and a single stationary patch with sharp boundaries is formed; see Fig. 5a obtained for $\mu = 0.005$ and $\epsilon = 0.001$. We will make a more careful insight into its properties in the next section.

In conclusion to this section, we also want to mention that as we observed in our numerical experiments, variation of the parameters γ and α does not bring any qualitative changes to the structure of the $\mu - \epsilon$ parametric plane as long as system's kinetics remains to be of excitable type.

3.2. Standing patches

Our numerical simulations show that for ϵ being either zero or only slightly greater than zero, the initial species outbreak always converge to a single stationary patch with a sharp boundary, i.e., a narrow transition region, separating the areas with high and low values of the prey density; see Fig. 5a. Outside the patch, with an increase in distance from the patch boundary, the prey density gradually approaches its equilibrium density $\bar{u}$. Inside the patch, the density reaches its minimum in the patch center and gradually increases toward the edge. The spatial distribution of predator is given by a slowly varying dome-shaped function.

The existence of patterns with sharp boundaries in a diffusion–reaction system with the diffusivity ratio $\epsilon \ll 1$ is a well-known phenomenon (cf. Fife, 1976; Mimura et al., 1980; Hastings et al., 1997; Hosseini, 2006). The boundary width is on the order of $\epsilon^{1/2}$ which apparently means that for $\epsilon = 0$ the density distribution becomes discontinuous: for a certain critical value v_* of the predator density, the trajectory in the phase plane of the system "jumps" from one stable branch of the isocline to the other; see Fig. 5b.

We want to emphasize here that patterns with the features described above is not just a mathematical toy, but is a phenomenon widely observed in various natural systems. In population dynamics, such pattern would correspond to a stationary outbreak of a species with very low diffusivity, its predatory or parasitoid species (with much higher diffusivity) being distributed smoothly across the patch border. Since spatial predator-prey systems with $\epsilon \ll 1$ are rather common in nature, cf. plants–insects or walking

[1] The situation is different if predation is ratio-dependent, cf. Alonso et al. (2002).

insects–birds interactions, it can be expected that this mechanism is in many cases responsible for formation of a patchy population structure. Indeed, Harrison (1997) observed similar standing patterns in the spatial distribution of the western tussock moth and eventually related it to the impact of a fast-moving parasitoid (Brodmann et al., 1997; Hastings et al., 1997). Therefore, it is important to better understand the properties of the corresponding species distribution such as what factors determine the height and width of the patch, what are the conditions for the density jump at the border, etc.

The first issue that we are going to address is what is the typical value v_* of the predator density corresponding to the patch boundary, i.e., the region with large gradient in the prey density. Taking into account that $v(x)$ is a slowly varying function (because $D_2/D_1 = 1/\epsilon \gg 1$), inside the transition region its value can be regarded as constant (Fife, 1976). The system (7–8) is then virtually reduced to a single equation for u and the usual condition for the front blocking can be applied, which results in the following equation for v_*:

$$\int_{u_1}^{u_2} P(u, v_*) = 0 \tag{20}$$

(Fife, 1976; also Murray, 1989) where function $P(u, v)$ describes the prey kinetics, cf. Eq. (9), and u_1 and u_2 are respectively the smallest and the biggest roots of the equation

$$P(u, v_*) = 0, \tag{21}$$

i.e., they are the values of the prey density on either side of the transition layer; thus, $\Delta u = u_2 - u_1$ gives the magnitude of the jump. Note that u_1 and u_2 can also be treated geometrically as the position of the intersection points between the isocline $v_1(u)$ and the horizontal line $v = v_*$.

Apparently, u_1 and u_2 depend on v_* which makes Eq. (20) analytically intractable for all interesting cases. It should be mentioned that the "equal areas rule" (i.e., that the areas between the line $v = v_*$ and the bends of the isocline $v_1(u)$ must be equal) does not apply here. However, one prediction that can be made from relation (20) is that the possible values of v_* are bound, $v_{\min} < v_* < v_{\max}$, where $v_{\min}$ and $v_{\max}$ are the values of the predator density corresponding to the minimum and the maximum of $v_1(u)$.

The magnitude Δu of the jump in the prey density can be estimated if we take into account the properties of specific parametrization. For $u \ll 1$, the isocline $v_1(u)$ can be approximated as

$$v_1(u) \simeq v_L(u) = \frac{\gamma(1-u)}{u}, \tag{22}$$

cf. (13). Note that $v_L(u) < v_1(u)$ for any u. For values of u in vicinity of $u = 1$, $v_1(u)$ can be approximated as

$$v_1(u) \simeq v_R(u) = \gamma\left(\alpha^2 + 1\right)(1-u). \tag{23}$$

Assuming $v_1(u)$ remains convex in the interval between its local maximum and $u = 1$, it is then obvious that $v_R(u) > v_1(u)$ for all u outside of some close vicinity of $u = 0$ (where $v_1(u)$ is unbounded), e.g., for $0 < \sigma \le u < 1$ where $\sigma \ll 1$ is a certain number.

The jump in the prey density at the patch border corresponds to the jump between the branches of the isocline, which we now can approximate as

$$\Delta u \approx u_R(v) - u_L(v) = \left(1 - \frac{v}{\gamma(\alpha^2+1)}\right) - \frac{\gamma}{\gamma+v}. \tag{24}$$

The value of the jump depends on $v = v_*$. Equation (24) is yet of little use because v_* cannot be calculated analytically. However, we can use it in order to estimate maximum possible value of the jump. Indeed, it is readily seen that $\Delta u(v)$, as given by (24), has a global maximum at

$$\tilde{v} = \gamma\left(\sqrt{\alpha^2+1} - 1\right) \tag{25}$$

so that having substituted (25) into (24), we obtain

$$(\Delta u)_{\max} = \left(1 - \frac{1}{\sqrt{\alpha^2+1}}\right)^2. \tag{26}$$

Relation (26) gives the maximum possible value of the jump in the prey density across the patch border. Note that it depends on the only parameter α.

Interestingly, it appears that the height and width of the stationary patch are not independent of each other. In order to show it, let us consider a patch of width $2L$ with the origin coinciding with the patch center. Outside the patch, as the distance from the patch boundary increases, the population densities gradually approach their equilibrium values $\bar{u}$ and $\bar{v}$. The functions $u(x)$ and $v(x)$ are the solution of the stationary system, i.e., system (7–8) where $\partial u/\partial t = \partial v/\partial t = 0$. Moreover, if we focus on the case $\epsilon = 0$, the system reduces to a single differential equation:

$$\frac{d^2v(x)}{dx^2} + \frac{u^2 v}{1+\alpha^2 u^2} - \mu v = 0, \tag{27}$$

where u and v are not independent but related by means of the equation for the prey isocline $P(u, v) = 0$, cf. (9–10).

Assuming that for any $|x| > L$ the population densities remain close to their equilibrium values, i.e., $u(x) = \bar{u} + \delta u(x)$ and $v(x) = \bar{v} + \delta v(x)$ where δu and δv are small, Eq. (27) can be linearized:

$$\frac{d^2\delta v(x)}{dx^2} + Q'_u \delta u + Q'_v \delta v = 0, \tag{28}$$

which after a little algebra, takes the following form:

$$\frac{d^2\delta v(x)}{dx^2} + \left(2\mu^2\bar{v}/\bar{u}^3\right)\delta u = 0. \tag{29}$$

To avoid tedious calculations, we assume that $\bar{u} \ll 1$, i.e., it lies in the range where the prey isocline can be approximated as $v_1(u) \approx \gamma/u$. From $P(\bar{u}+\delta u, \bar{v}+\delta v) = 0$, we then obtain

$$\delta u(x) \approx -\left(\gamma/\bar{v}^2\right)\delta v(x) \tag{30}$$

so that Eq. (29) turns into

$$\frac{d^2\delta v(x)}{dx^2} = \Gamma^2 \delta v, \tag{31}$$

where $\Gamma^2 = 2\gamma\mu^2/(\bar{v}\bar{u}^3) \approx 2\mu(1-\alpha^2\mu)$. Correspondingly, the predator density profile outside the patch is given as

$$v(x) = \bar{v} + \delta v \approx \bar{v} + (v_* - \bar{v}) \exp\big[-\Gamma\big(|x| - L\big)\big], \tag{32}$$

where $|x| \geq L$.

Equation (32) can then be used to calculate the flux of the population density through the patch boundary:

$$2J = 2\left|\frac{dv}{dx}\right| = 2\Gamma(v_* - \bar{v}). \tag{33}$$

The idea of our approach is that because the patch is stationary, the diffusion flux at the patch boundary must be balanced with the population growth inside the patch. Having integrated Eq. (27) from $-L$ to L, we obtain:

$$\int_{-L}^{L} \left(\frac{u^2 v}{1+\alpha^2 u^2} - \mu v\right) dx = 2J = 2\Gamma(v_* - \bar{v}). \tag{34}$$

Now we can make use of the heuristic observation that inside the patch, the population density varies insignificantly, cf. Fig. 5. Considering $u \approx u_2$ and $v \approx v_*$, from (34), we arrive at

$$L v_* \left(\frac{u_2^2}{1+\alpha^2 u_2^2} - \mu\right) \cong \Gamma(v_* - \bar{v}). \tag{35}$$

For the specific parametrization of the functional responses, see Eqs. (7–8); an interesting parameter range (when the prey isocline is N-shaped) is reached for $\alpha \gg 1$ while the prey density inside the patch appears to be on the order of unity. In this case, Eq. (35) takes somewhat simpler form:

$$L v_* \left(\frac{1}{\alpha^2} - \mu\right) \cong \Gamma(v_* - \bar{v}) \tag{36}$$

and finally,

$$L v_* \cong 2\mu\alpha^2(v_* - \bar{v}). \tag{37}$$

Although (37) is an estimate and not an exact relation, it clearly means that the patch size and the typical population density inside are not independent of each other. In particular, relation (37) rules out the situations that both the size and height of the patch are either very large or very small.

3.3. Pattern formation in 2-D case

Understanding of the dynamics of the predator-prey system with one spatial dimension is useful and instructive, yet the dynamics of real population communities more typically takes place in a two dimensional spatial domain. In this section, we will try to reveal to what extent the results of the 1-D study can be extended onto the corresponding 2-D system. By means of numerical simulations, we will study patterns of dynamics arising in the 2-D excitable system (5–6) and construct the corresponding map in $\mu - \epsilon$ parametric plane keeping the values of other parameters fixed at the same hypothetical values as in the 1-D case (i.e., $\gamma = 1$ and $\alpha = 10$).

Numerical simulations in a two-dimensional system are much more resource-consuming; therefore, we are not able to restore the boundaries of different domains as accurately as it was done in the 1-D case; see Fig. 2. Instead, we have varied ϵ by small steps for several selected values of μ. The results are shown in Fig. 6 where different symbols correspond to different regimes are discussed below.

In the case of a fast dispersing prey (large ϵ), we found that a supercritical excitation (18–19) of the system results in the formation and expansion of concentric rings of high species density. In the $\mu - \epsilon$ diagram of Fig. 6, the corresponding domain is shown by the circles. The predator is not able to block the spread of the outbreak. The wave of the high density travels through the whole domain, and eventually, out of the system. In the wake of the expanding ring, the distributions of species become spatially homogeneous

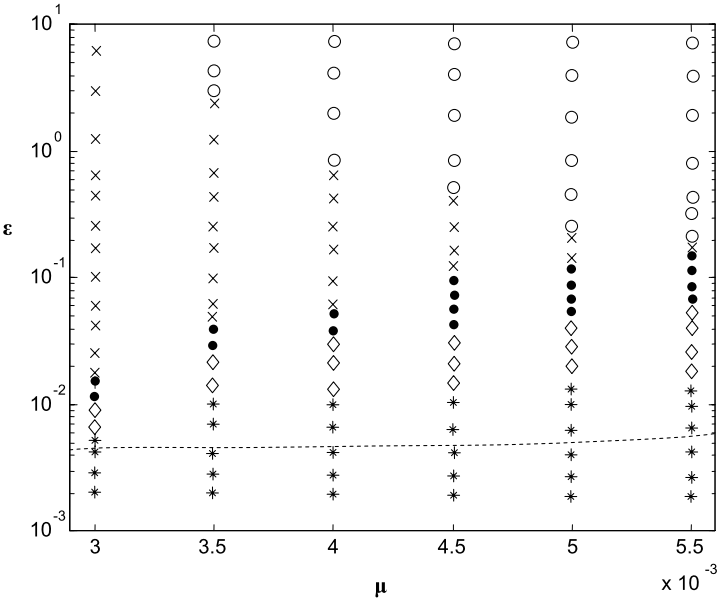

Fig. 6 A map in the $\mu - \epsilon$ parameter plane obtained for $\gamma = 1$ and $\alpha = 10$. Different symbols stand for different dynamical regimes of the 2-D system (5–6): circles for ring-shaped pattern, crosses for the dynamical localization of the rings, bullets for the patchy spread with rare patch density (Fig. 7), diamonds for the patchy spread with high patch density (Fig. 8), and asterisk for the formation of labyrinthine patterns (Fig. 9).

again, with the population densities being at their steady state values. On the whole, this regime looks like a natural extension of the traveling pulses scenario onto a 2-D system.

For a decrease in ϵ, however, rings blocking becomes possible. The predator catches up with the prey and brings the prey outbreak down. The corresponding parameter values in Fig. 6 are marked by the crosses. Note that the relaxation of the initial outbreak to the spatial homogeneity takes place via a scenario which is rather different from the one observed in the 1-D case. In the 2-D system, instead of a monotonous decay of the population density inside the ring (as it might have been expected basing on the 1-D results, cf. Fig. 3b), the ring is first split into an ensemble of separate patches. For a period of time, the patches exhibit a complicated dynamics of irregular motion and interaction. Finally, however, the patches go extinct and the homogeneous distribution of species is restored. The patchy dynamics becomes more prominent and takes a longer time for smaller values of ϵ, i.e., when the parameters approach the lower boundary of the cross-marked domain.

A slower moving prey (i.e., for smaller values of ϵ) regain its ability to escape from the predator, so that the initial outbreak would never decay and the spatial homogeneity is never restored. Particular scenarios can be different. Parameters marked by the bullets (see Fig. 6) correspond to the patchy spatial spread of the initially localized outbreak. A typical pattern of such dynamics is shown in Fig. 7 (obtained for $\mu = 0.005, \epsilon = 0.1$ and the initial conditions (18–19) with $\Delta_x = 3, \Delta_y = 9, a = b = 0.375$, $x_0 = y_0 = 125$ and $V_0 = 12$). Only the distribution of prey is shown; the predator density shows similar features. At a very early stage of the patchy spread, a continuous propagating front is formed, similar to what would happen in the regime of expanding rings. However, the front soon breaks to pieces, thus creating an ensemble of separate patches. A further spatial spread of the outbreak takes place via irregular movement of the individual patches and groups of patches, and a continuous front never reappears. The patches move, merge, disappear, split, and produce new patches, etc. After the patches invade the whole area, the spatial distribution of species at any time remains qualitatively similar to the one shown for $t = 2500$, although the position and shape of specific patches change in the course of time. This type of spread (also known as "patchy invasion") has been previously observed and studied in much detail for a predator-prey system with somewhat different properties; see Petrovskii et al. (2002, 2005), Morozov et al. (2008, 2006), Malchow et al. (2008), Sherratt and Smith (2008).

With a decrease in ϵ, the speed of the patchy spread becomes slower and the patches themselves become distinctly round-shaped. With a further decrease, though, their shape becomes elongated and the separate patches tend to give way to groups of patches, cf. Fig. 8 obtained for $\mu = 0.005$ and $\epsilon = 0.03$ and the same initial conditions as in Fig. 7. The pattern as a whole is now more densely packed. In the diagram of Fig. 6, the corresponding domain is marked by the diamonds. We want to note, however, that the difference between the patterns shown in Figs. 7 and 8 is quantitative rather than qualitative, and the transition between the two examples of patchy spread is gradual and not related to any bifurcation. Correspondingly, the boundary between the bullet-marked and the diamond-marked parameter domains is rather conventional.

For a further decrease of ϵ, the speed of the patchy spread becomes even slower. The patches now create a sprout-shape structure and most of them are merged together along a complicated curve, thus creating the so-called "labyrinthine patterns" (Muratov and Osipov, 1996a, 1996b). The corresponding domain in Fig. 6 is marked by asterisks. Typical snapshots for this case are shown in Fig. 9 obtained for $\mu = 0.005$ and $\epsilon = 0.01$. After the

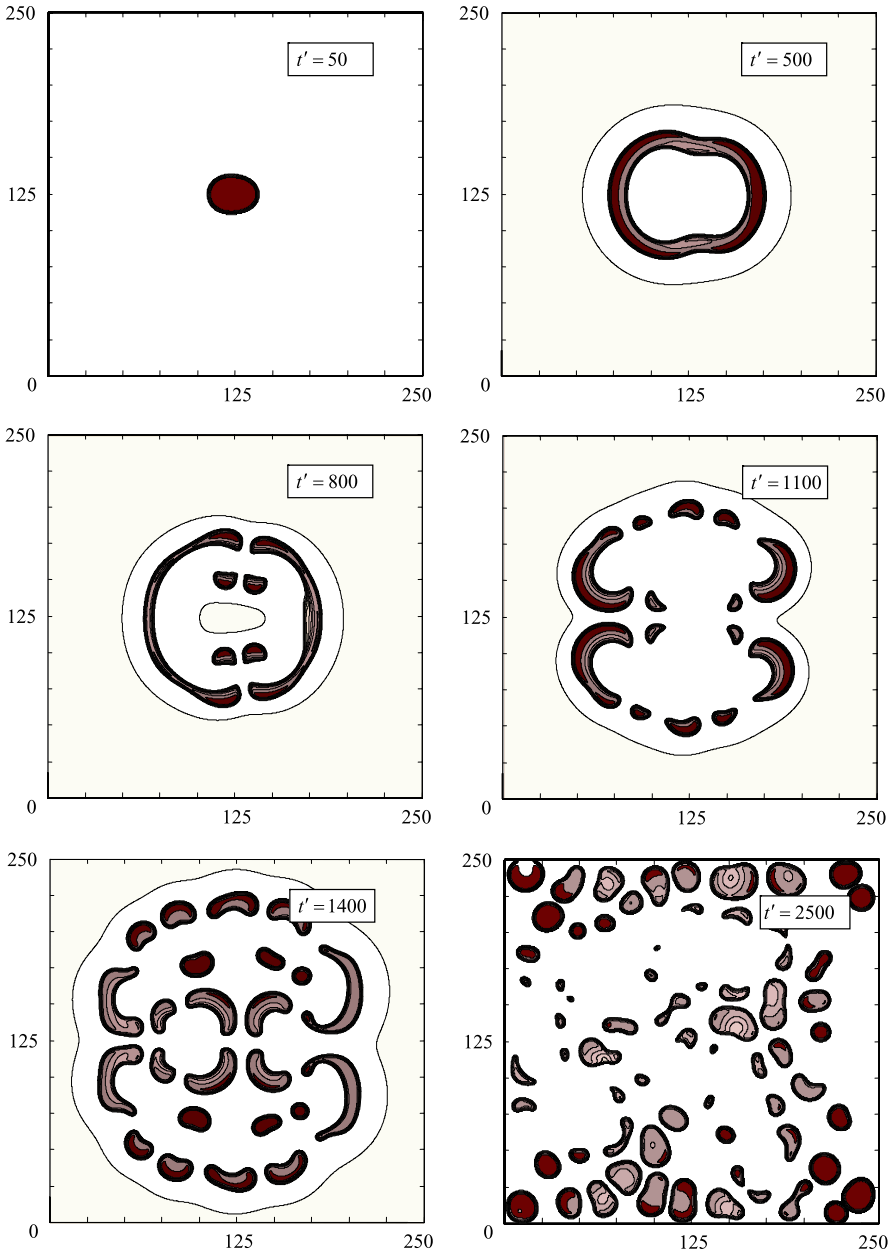

Fig. 7 Isoclines of the prey density in the 2-D system (5–6): Formation of an irregular spatial pattern for parameters $\mu = 0.005$ and $\epsilon = 0.1$. The thick lines correspond to the areas of a large gradient in the population density. The thin front line is the first isocline corresponding to only a slight deviation from the steady state values $\bar{u}$ and $\bar{v}$; hence, it shows the position of the "precursor" of the spreading perturbation.

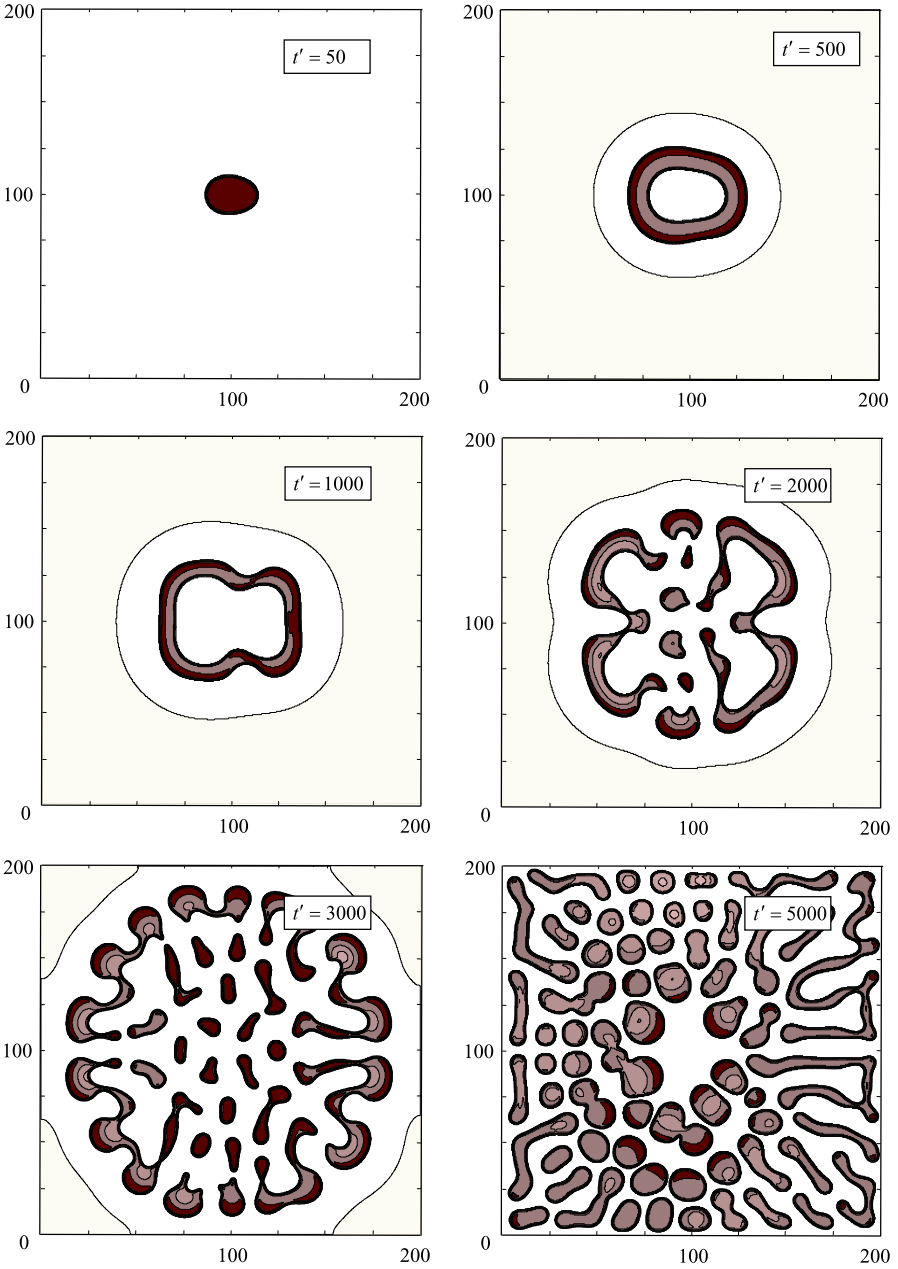

Fig. 8 Snapshots (isoclines) of the prey density in the 2-D system (5–6): Formation of an irregular spatial pattern for parameters $\mu = 0.005$ and $\epsilon = 0.03$.

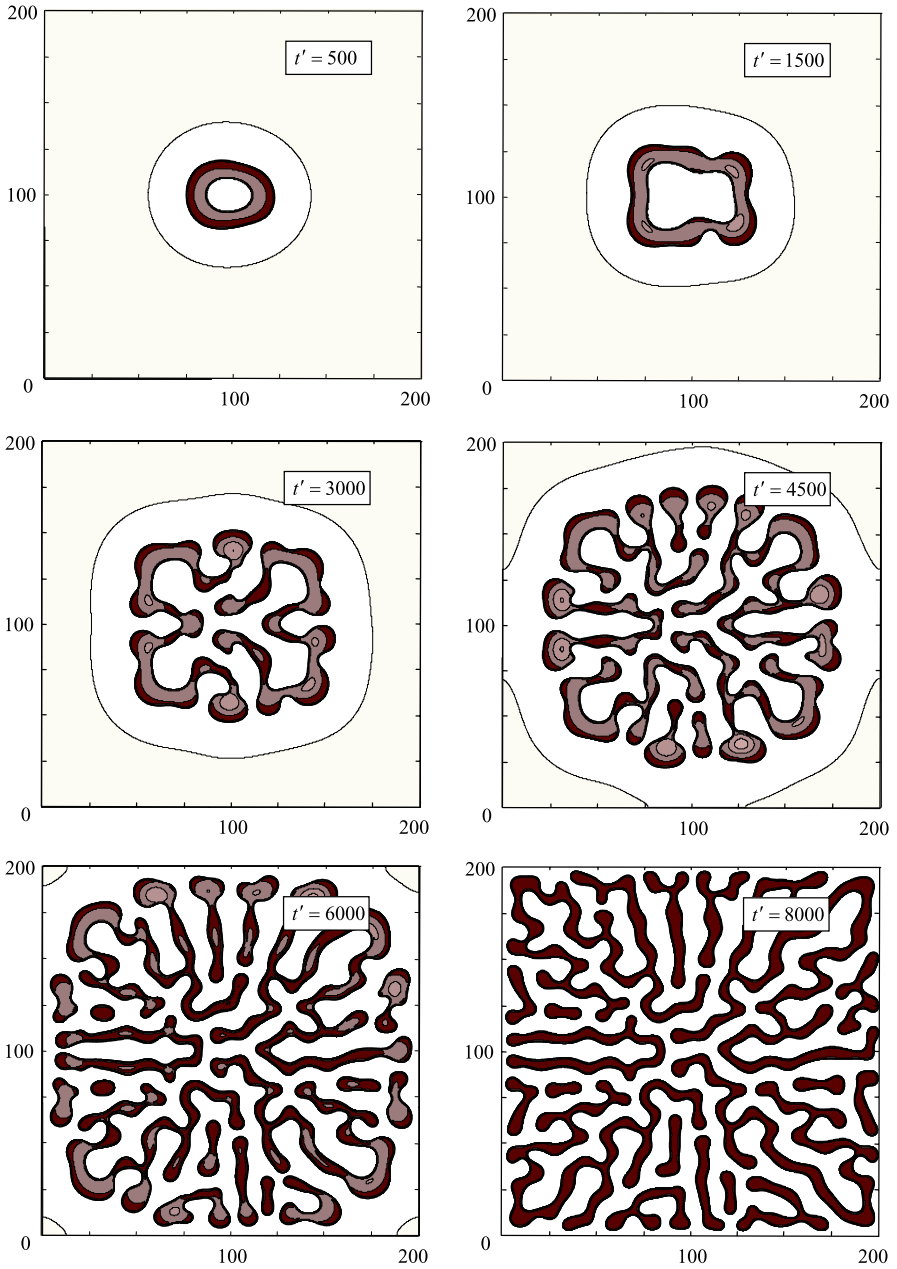

Fig. 9 Snapshots (isoclines) of the population density in the 2-D system (5–6): Formation of a labyrinthine spatial pattern for parameters $\mu = 0.005$ and $\epsilon = 0.01$.

patches have invaded over the whole spatial domain, they slowly change their shape and position. For very small values of ϵ (below the dashed curve in Fig. 6), the labyrinthine structures become stationary.

Interestingly, in the 2-D case, formation of solitary stationary patches (i.e., the 2-D analogue of the pattern shown in Fig. 5) in the considered domain of square shape is suppressed. We have found that the size of the habitat plays a crucial role. In particular, we did not find the stationary structures for $L < 300$. Numerical simulations show that in the 2-D case, for small values of ϵ, every supercritical initial disturbance (19) results in a spread of labyrinthine structures (even for initial perturbations with a round boundary). However, for a square-shaped habitat of sufficiently large size (e.g., $L = 600$), we did find round-shaped stationary patches. Note that numerical simulations show that in the 2-D case with a radial symmetry (for a round-shaped habitat of radius R), formation of solitary patches can take place for somewhat smaller sizes of the habitat ($R > 100$) for μ and ϵ approximately situated below the dashed curve in Fig. 6.

4. Concluding remarks

In this paper, we have considered the problem of harmful species management when a pest is kept under control by its predator. The predator trophic response was assumed to be of Holling type III, which makes the system's kinetics excitable. In a certain parameter range, the system was shown to have a unique stable steady coexistence state, where the prey density is significantly lower than it would have been without the impact of predator. Although at the first sight it may be regarded as a successful implementation of the biological control strategy, the question remains as to how robust this situation is with respect to various disturbances.

Here, we have been particularly interested in a situation when this predator-prey system in its stable steady state experiences a finite local perturbation to the population density. In a real-world system, such a perturbation may come as a result of fluctuations in the weather conditions, spatially inhomogeneous demographic, or environmental noise, etc. It is well known (cf. Truscott and Brindley, 1994a, 1994b) that the corresponding nonspatial system exhibits criticality in its behavior. While small (subcritical) perturbations decay exponentially, perturbations of overcritical magnitude result in a species outbreak, so that the system returns to its equilibrium state through a long-living transient dynamics with high values of the prey density. Our main goal was to reveal how the system's dynamics can possibly change when space is taken into account.

It should be mentioned here that Holling type III tropical response is widely accepted to originate in the specifics of the predator's feeding behavior when it either changes its foraging strategy or switches to some alternative resource(s) (not included into the model explicitly) if the density of the prey drops too low. The existence of such an alternative prey may partially account for the very high predator density at the equilibrium compare to the density of the prey, cf. Fig. 1. Moreover, variations of alternative prey abundance can be an additional source of spatiotemporal perturbations in predator density, which can result in breakdown of the spatially homogeneous population distribution.

The spatiotemporal dynamics of the predator-prey system triggered by a localized perturbation was studied by means of extensive computer simulations. The following results have been obtained:

1. For an initial perturbation of a small magnitude, both the spatial and nonspatial systems promptly return into the equilibrium state. However, for a larger (overcritical) perturbation, there is a crucial difference between the properties of a nonspatial excitable system and its spatial counterpart. While the nonspatial system eventually returns into its equilibrium state (although being preceded by a long excursion over the phase space and high prey density), the dynamics of the spatially extended system can be self-sustained. Having been once driven away by a local population outbreak, the system never returns to its stable spatially-homogeneous equilibrium state. Instead, it evolves into formation of complex spatiotemporal patterns.
2. On the whole, the spatiotemporal system dynamics appears to be rather rich, and a wide variety of dynamical regimes has been observed. By means of "scanning" the parameter space of the system, we revealed its structure and identified the parameter domains corresponding to different dynamical regimes. In particular, we found that a typical scenario of successful biological control in the spatially explicit excitable system is the "dynamical localization" of the traveling pulses (cf. Fig. 3b): the predator catch-up with the prey, blocks the pulse propagation, and then promptly brings the prey density down to its equilibrium value.
3. The lower is the predator mortality rate μ, the wider is the range of ϵ corresponding to successful biological control; see domain 2 in Fig. 2 and the cross-marked domain in Fig. 6. That seems to agree with an intuitive expectation that a stronger predator should be more effective as a controlling factor.
4. Rather counter-intuitively, however, both slow moving ($\epsilon > 1$) and fast moving ($\epsilon \ll 1$) predator appears to be unable to keep the prey under control. While for $\epsilon \sim 1$ or larger a common pattern of system's dynamics is traveling pulses (in the 1-D case) or expanding rings (in the 2-D case), for $\epsilon \ll 1$, the typical pattern is a standing patch (see Section 3.2). Therefore, in the latter case, predator is able to localize the outbreak, but is not able to bring it down, so that the spatial homogeneity is never restored.
5. The parameter ranges of successful biological control appear to be different for 1-D and 2-D systems, the conditions of successful control being less restrictive in the 1-D case. The system's dimensionality has therefore a noticeable impact on the robustness of the biological control.

We want to mention that the simple model (5–6) is of course only a caricature of very complicated processes going in ecosystems. Nevertheless, it appears capable of catching some essential properties of real population communities and patterns of their dynamics such as, for instance, formation of a standing patch in the case of a pest with a low diffusivity ($\epsilon \ll 1$) (Hastings et al., 1997) and formation of patchy structures or stripy labyrinthine structures (see Figs. 7 and 9). In particular, patchy and stripy structures are typical vegetation patterns in semiarid regions[2], e.g., see White (1970) and Belsky (1986).

The results of our study lead to a few conclusions. Firstly, we want to emphasize that if a theoretical study is done using a nonspatial model, its results should be used with great care as the dynamics of the corresponding spatial system can be qualitatively different. In particular, a predator-prey system with excitable dynamics was earlier used as a model

[2]The semiarid vegetation patterns sometimes exhibit spatial anisotropy due to an environmental forcing (cf. Couteron and Lejeune, 2001) which is not included into our model.

for spontaneous phytoplankton outbreak or "bloom" (also known as a "red tide"); see Truscott and Brindley (1994a, 1994b). Correspondingly, it was concluded that termination of bloom is just an intrinsic feature of the system when the system's trajectory leaves the isocline and the density of prey (phytoplankton, in this context) promptly approaches its equilibrium value (see the upper part of Fig. 1). However, the results of our study point out that this conclusion may be wrong. An initial outbreak should more likely result in formation of a self-sustained spatially heterogeneous structure. (Interestingly, a red tide with a distinctive patchy structure is indeed a frequently observed phenomenon, e.g., see Cosper et al., 1989; Smayda and Shimuza, 1993.) Termination of the bloom then should be ascribed to the impact of some external factors (such as, for instance, depletion of oxygen) that are not included into the baseline predator-prey model.

Another and possibly more important message from this study should be addressed to decision-makers in the pest control management. When choosing a species that will act as the controlling agent for a given pest, one might wish to take into consideration that a predator with the diffusivity too high compared to the diffusivity of the pest may appear to be ineffective and/or not robust with respect to environmental and demographic perturbations; see item #4 from the list above. Interestingly, a similar conclusion was made by Sapoukhina et al. (2003) in another theoretical study concerned with different aspects of the predator-prey dynamics. It indicates that the optimality of predator's diffusivity as a controlling factor is a real issue (cf. Crawley, 1997). We want to mention here that this theoretical prediction is in a very good agreement with some biological data: Indeed, it was proved by Ferran et al. (1998) that a flightless strain of the ladybird *Harmona axyridis* is a much more effective biological agent to control aphids than the common strain.

References

Alonso, D., Bartumeus, F., Catalan, J., 2002. Mutual interference between predators can give rise to Turing spatial patterns. Ecology 83, 28–34.

Belsky, A.J., 1986. Population and community processes in a mosaic grassland in the Serengeti, Tanzania. J. Ecol. 74, 841–856.

Briggs, C.J., Hoopes, M.F., 2004. Stabilizing effects in spatial parasitoid-host and predator-prey models: a review. Theor. Popul. Biol. 65, 299–315.

Brodmann, P.A., Wilcox, C.V., Harrison, S., 1997. Mobile parasitoids may restrict the spatial spread of an insect outbreak. J. Anim. Ecol. 66, 65–72.

Cosper, E.M., Bricelj, V.M., Carpenter, E.J., 1989. Novel Phytoplankton Blooms. Coastal and Estuarine Studies, vol. 35. Springer, Berlin.

Couteron, P., Lejeune, O., 2001. Periodic spotted patterns in semi-arid vegetation explained by a propagation-inhibition model. J. Ecol. 89, 616–628.

Crawley, M.J., 1997. Plant-herbivore dynamics. In: Crawley, M.J. (Ed.), Plant Ecology, pp. 463–465. Blackwell, Oxford.

Edwards, A.M., Brindley, J., 1999. Zooplankton mortality and the dynamical behavior of plankton population models. Bull. Math. Biol. 61, 202–239.

Ermentrout, B., Chen, X., Chen, Z., 1997. Transition fronts and localized structures in bistable reaction-diffusion equations. Physica D 108, 147–167.

Fagan, W.F., Lewis, M.A., Neubert, M.G., van den Driessche, P., 2002. Invasion theory and biological control. Ecol. Lett. 5, 148–157.

Ferran, A., Guige, L., Tourniaire, R., Gambier, J., Fournier, D., 1998. An artificial non-flying mutation to improve the efficiency of the ladybird Harmonia axyridis in the biological control of aphids. Biocontrol 43, 53–64.

Fife, P.C., 1976. Pattern formation in reacting and diffusing systems. J. Chem. Phys. 64, 554–564.

Franks, P., 2001. Phytoplankton blooms in a fluctuating environment: the roles of plankton response time scales and grazing. J. Plankt. Res. 23, 1433–1441.
Gurney, W.S.C., Veitch, A.R., Cruickshank, I., McGeachin, G., 1998. Circles and spirals: population persistence in a spatially explicit predator-prey model. Ecology 79, 2516–2530.
Harrison, S., 1997. Persistent localized outbreaks in the western tussock moth (Orgyia vetusta): the roles of resource quality, predation and poor dispersal. Ecol. Entomol. 22, 158–166.
Hajek, A., 2004. Natural Enemies: An Introduction to Biological Control. Cambridge University Press, Cambridge.
Hastings, A., Harisson, S., McCann, K., 1997. Unexpected spatial patterns in an insect outbreak match a predator diffusion model. Proc. R. Soc. Lond. B 264, 1837–1840.
Hosseini, P.R., 2006. Pattern formation and individual-based models: the importance of understanding individual-based movement. Ecol. Model. 194, 357–371.
Hunter, A.F., Dwyer, G., 1998. Outbreaks and interacting factors: insect population explosions synthesized and dissected. Integr. Biol. 1, 166–177.
Krischer, K., Mikhailov, A., 1994. Bifurcation to travelling spots in reaction-diffusion systems. Phys. Rev. Lett. 73, 3165–3168.
Lindner, B., García-Ojalvo, J., Neiman, A., Schimansky-Geier, L., 2004. Effects of noise in excitable systems. Phys. Rep. 392, 321–424.
Lotka, A.J., 1925. Elements of Physical Biology. Williams and Wilkins, Baltimore.
Ludwig, D., Jones, D.D., Holling, C.S., 1978. Qualitative analysis of insect outbreak systems: the spruce budworm and forest. J. Anim. Ecol. 47, 315–332.
Malchow, H., Petrovskii, S.V., Venturino, E., 2008. Spatiotemporal Patterns in Ecology and Epidemiology: Theory, Models, and Simulations. Chapman & Hall/CRC Press, London.
May, R.M., 1974. Stability and Complexity in Model Ecosystems. Princeton University Press, Princeton.
McEvoy, P., Cox, C., Coombs, E., 1991. Successful biological control of Ragwort, Senecio Jacobaea, by introduced insects in Oregon. Ecol. Appl. 1, 430–442.
Mendel, Z., Assael, F., Zeidan, S., Zehavi, A., 1998. Classical biological control of Palaeococcus fuscipennis (Burmeister) (Homoptera: Margarodidae) in Israel. Biol. Control 12, 151–157.
Mimura, M., Tabata, M., Hosono, Y., 1980. Multiple solutions of two-point boundary value problem of Neumann type with a small parameter. SIAM J. Math. Anal. 11, 613–631.
Morozov, A.Y., Petrovskii, S.V., Li, B.-L., 2006. Spatiotemporal complexity of the patchy invasion in a predator-prey system with the Allee effect. J. Theor. Biol. 238, 18–35.
Morozov, A.Y., Ruan, S., Li, B.L., 2008. Patterns of patchy spread in multi-species reaction–diffusion models. Ecol. Complex. 5, 313–328.
Muratov, C.B., 1996. Self-replication and splitting of domain patterns in reaction–diffusion systems with the fast inhibitor. Phys. Rev. E 54, 3369–3376.
Muratov, C.B., Osipov, V.V., 1996a. General theory of instabilities for patterns with sharp interfaces in reaction–diffusion systems. Phys. Rev. E 53, 3101–3116.
Muratov, C.B., Osipov, V.V., 1996b. Scenarios of domain pattern formation in a reaction–diffusion system. Phys. Rev. E 54, 4860–4879.
Murray, J.D., 1989. Mathematical Biology. Springer, Berlin.
Nisbet, R.M., Gurney, W.S.C., 1982. Modelling Fluctuating Populations. Wiley, Chichester.
Pascual, M., 1993. Diffusion-induced chaos in a spatial predator-prey system. Proc. R. Soc. Lond. B 251, 1–7.
Pascual, M., Caswell, H., 1997. Environmental heterogeneity and biological pattern in a chaotic predator-prey system. J. Theor. Biol. 185, 1–13.
Pearson, J.E., 1993. Complex patterns in a simple system. Science 261, 189–192.
Petrovskii, S.V., Li, B.-L., 2001. Increased coupling between sub-populations in a spatially structured environment can lead to population outbreaks. J. Theor. Biol. 212, 549–562.
Petrovskii, S.V., Li, B.-L., 2006. Exactly Solvable Models of Biological Invasion. Chapman & Hall/CRC Press, London.
Petrovskii, S.V., Malchow, H., 1999. A minimal model of pattern formation in a prey-predator system. Math. Comput. Model. 29, 49–63.
Petrovskii, S.V., Malchow, H., 2001. Wave of chaos: new mechanism of pattern formation in spatio-temporal population dynamics. Theor. Popul. Biol. 59, 157–174.
Petrovskii, S.V., Morozov, A.Y., Venturino, E., 2002. Allee effect makes possible patchy invasion in a predator-prey system. Ecol. Lett. 5, 345–352.

Petrovskii, S.V., Malchow, H., Hilker, F., Venturino, E., 2005. Patterns of patchy spread in deterministic and stochastic models of biological invasion and biological control. Biol. Invasions 7, 771–793.
Room, P.M., Harley, K.L.S., Forno, I.W., Sands, D.P.A., 1981. Successful biological control of the floating weed salvinia. Nature 294, 78–80.
Sapoukhina, N., Tyutyunov, Y., Arditi, R., 2003. The role of prey-taxis in biological control: a spatial theoretical model. Am. Nat. 162, 61–76.
Scheffer, M., 1991. Fish and nutrients interplay determines algal biomass: a minimal model. Oikos 62, 271–282.
Scheffer, M., 1998. Ecology of Shallow Lakes. Chapman & Hall, London.
Segel, L.A., Jackson, J.L., 1972. Dissipative structure: an explanation and an ecological example. J. Theor. Biol. 37, 545–559.
Sherratt, J.A., Lewis, M.A., Fowler, A.C., 1995. Ecological chaos in the wake of invasion. Proc. Natl. Acad. Sci. USA 92, 2524–2528.
Sherratt, J.A., Smith, M.J., 2008. Periodic travelling waves in cyclic populations: field studies and reaction–diffusion models. Interface 5, 483–505.
Shigesada, N., Kawasaki, K., 1997. Biological Invasions: Theory and Practice. Oxford University Press, Oxford.
Smayda, T.J., Shimuza, Y. (Eds.), 1993. Toxic Phytoplankton Blooms in the Sea. Elsevier, Amsterdam.
Thomas, J., 1995. Numerical Partial Differential Equations: Finite Difference Methods. Texts in Applied Mathematics, vol. 22. Springer, New York.
Truscott, J.E., Brindley, J., 1994a. Ocean plankton populations as excitable media. Bull. Math. Biol. 56, 981–998.
Truscott, J.E., Brindley, J., 1994b. Equilibria, stability and excitability in a general class of plankton population models. Philos. Trans. R. Soc. Lond. A 347, 703–718.
Volterra, V., 1926. Fluctuations in the abundance of a species considered mathematically. Nature 118, 558–560.
White, L.P., 1970. Brousse tigrée patterns in Southern Niger. J. Ecol. 58, 549–553.